the plant journal

SEB SOCIETY FOR EXPERIMENTAL BIOLOGY

The Plant Journal (2022) **112,** 1396–1412 doi: 10.1111/tpj.16018

Genotype-dependent changes of cell wall composition influence physiological traits of a long and a non-long shelf-life tomato genotypes under distinct water regimes

Margalida Roig-Oliver[1,*], Mateu Fullana-Pericàs[1], Josefina Bota[1] and Jaume Flexas[1,2]

[1]*Research Group on Plant Biology under Mediterranean Conditions, Departament de Biologia, Universitat de les Illes Balears (UIB) – Agro-Environmental and Water Economics Institute (INAGEA), Carretera de Valldemossa Km 7.5, 07122, Palma, Illes Balears, Spain, and*

[2]*King Abdulaziz University, P.O. Box 80200, Jeddah 21589, Saudi Arabia*

Received 22 July 2022; revised 22 October 2022; accepted 26 October 2022; published online 30 October 2022.
*For correspondence (e-mail margaroig93@gmail.com).

SUMMARY

Water shortage strongly affects plants' physiological performance. Since tomato (*Solanum lycopersicum*) non-long shelf-life (nLSL) and long shelf-life (LSL) genotypes differently face water deprivation, we subjected a nLSL and a LSL genotype to four treatments: control (well watering), short-term water deficit stress at 40% field capacity (FC) (ST 40% FC), short-term water deficit stress at 30% FC (ST 30% FC), and short-term water deficit stress at 30% FC followed by recovery (ST 30% FC-Rec). Treatments promoted genotype-dependent elastic adjustments accompanied by distinct photosynthetic responses. While the nLSL genotype largely modified mesophyll conductance (g_m) across treatments, it was kept within a narrow range in the LSL genotype. However, similar g_m values were achieved under ST 30% FC conditions. Particularly, modifications in the relative abundance of cell wall components and in sub-cellular anatomic parameters such as the chloroplast surface area exposed to intercellular air space per leaf area (S_c/S) and the cell wall thickness (T_{cw}) regulated g_m in the LSL genotype. Instead, only changes in foliar structure at the supra-cellular level influenced g_m in the nLSL genotype. Even though further experiments testing a larger range of genotypes and treatments would be valuable to support our conclusions, we show that even genotypes of the same species can present different elastic, anatomical, and cell wall composition-mediated mechanisms to regulate g_m when subjected to distinct water regimes.

Keywords: bulk modulus of elasticity, cell wall composition, cell wall thickness, long shelf-life genotypes, mesophyll conductance, non-long shelf-life genotypes, tomato, water deficit stress.

INTRODUCTION

Water scarcity is one of the most relevant abiotic stresses limiting photosynthesis and, thus, plant growth and productivity (Chaves et al., 2009; Flexas et al., 2004; Nadal & Flexas, 2019). In the present scenario of climate change, which is mainly characterised by increased temperatures and large reductions in the water supply, agriculture is one of the most affected sectors (Morison et al., 2008). Together with the desertification of several regions, the global population is predicted to increase during the next decades, enhancing the demand for crop production (Schultz, 2016; Tilman et al., 2002). Since one of the major challenges for plant physiology is to improve crops' productivity (Evans, 1997; Long et al., 2006; Wu et al., 2019), there is a need to select drought-resistant genotypes to ensure food requirements can be met (Mickelbart et al., 2015).

Tomato (*Solanum lycopersicum* L.) is among the most produced and consumed horticultural crops worldwide, and more than 83 000 tomato genotypes are available (FAO, 2021). During the past centuries, tomato has undergone diverse cultivation practices partially based on the conditions of each region, leading to the distinctive adaptation of different landraces to specific areas (Bota et al., 2014; Cebolla-Cornejo et al., 2013; Conesa et al., 2020; Cortés-Olmos et al., 2015; Flores et al., 2017; Fullana-Pericàs et al., 2017, 2019). Particularly, the Western Mediterranean long shelf-life (LSL) tomato landraces have been traditionally selected according to their fruit phenotype, which remains without signs of deterioration for more than 6–12 months

after harvest (Bota et al., 2014; Conesa et al., 2014; Manzo et al., 2018; Saladié et al., 2007). Besides this particularity regarding fruit conservation, LSL genotypes in their vegetative state have also been related to drought tolerance because of molecular, morphological, physiological, and biochemical adaptations (Fullana-Pericàs et al., 2017, 2019; Galmés et al., 2011, 2013; Tranchida-Lombardo et al., 2018). Specifically, Galmés et al. (2011) demonstrated that LSL genotypes exhibited higher intrinsic water use efficiency (WUE_i, i.e., increased net CO_2 assimilation [A_N]/stomatal conductance [g_s] ratio) than non-long shelf-life (nLSL) ones when subjected to water deficit stress, minimising reductions in A_N as compared to g_s declines. In fact, this enhanced WUE_i has been correlated positively with the ratio between mesophyll and stomatal conductances (i.e., the g_m/g_s ratio), with stomatal traits and distribution, and with mesophyll anatomical properties (Conesa et al., 2020; Fullana-Pericàs et al., 2017; Galmés et al., 2011, 2013). Besides the gas exchange perspective, drought also induced changes in the foliar structure and in leaf water relations parameters, particularly in the leaf mass per area (LMA) and in the bulk modulus of elasticity (ε) (Galmés et al., 2011). Apart from the existence of those strategies exclusively related to photosynthetic adjustments, it is still unknown if other traits could distinctively affect the physiological performance of tomato LSL and nLSL genotypes subjected to water deficit stress (Conesa et al., 2020).

Recent studies have shown that modifications in cell wall composition determined photosynthesis performance, leaf water relations, and/or anatomical adjustments in different species subjected to contrasting abiotic conditions such as water deprivation (Clemente-Moreno et al., 2019; Roig-Oliver, Bresta, et al., 2021; Roig-Oliver, Fullana-Pericàs, et al., 2021; Roig-Oliver, Bresta, Nadal, et al., 2020; Roig-Oliver, Nadal, Bota, et al., 2020; Roig-Oliver, Nadal, Clemente-Moreno, et al., 2020). From these studies, it appears that each species presented changes in g_m, ε, and cell wall thickness (T_{cw}), which were differently related to modifications in specific cell wall components, suggesting that these relationships could be species-specific (Flexas et al., 2021). Nevertheless, to the best of our knowledge, only the study by Ye et al. (2020) evaluated how changes in cell wall composition influenced g_m and T_{cw} in distinct genotypes of the same species. Particularly, they did not find correlations among these parameters analysing eight rice (*Oryza sativa*) genotypes subjected to well-watering conditions. However, grasses present a very characteristic cell wall composition within angiosperms (Carpita, 1996; Carpita & McCann, 2002), which makes their results difficult to extrapolate to other species. Since water deprivation affects cell wall composition (Clemente-Moreno et al., 2019; Nadal et al., 2020; Roig-Oliver, Bresta, Nadal, et al., 2020; Roig-Oliver, Nadal, Bota, et al., 2020; Roig-Oliver, Nadal, Clemente-Moreno, et al., 2020; Roig-Oliver, Bresta, et al., 2021; Roig-Oliver, Fullana-Pericàs, et al., 2021; Rui & Dinneny, 2019; Sweet et al., 1999; Tenhaken, 2015) and induces changes in photosynthesis, leaf water relations, and anatomical characteristics even at the genotype level (Fullana-Pericàs et al., 2017, 2019; Galmés et al., 2011, 2013), we tested a tomato LSL and a nLSL genotype subjected to distinct levels of water shortage. Additionally, a recovery treatment was applied to separate the commonly proportional responses of g_s and g_m (Flexas et al., 2013). Thus, our hypothesis is that T_{cw} and composition change more plastically in the LSL genotype in response to distinct water availability treatments, differentially determining g_m, ε, and T_{cw} in both genotypes.

RESULTS

Plant water status

Both genotypes presented non-significant differences in pre-dawn leaf water potential (Ψ_{pd}) between control (CL) and short-term water deficit stress at 40% field capacity (ST 40% FC) conditions (Table 1). However, an almost 4-fold decrease was detected under ST 30% FC conditions in both cases (Table 1). Although the nLSL genotype presented significant reductions in midday leaf water potential (Ψ_{md}) under ST 40% FC conditions as compared to CL levels (−0.96 ± 0.03 and −0.40 ± 0.01 MPa, respectively), these decreases were only significant under ST 30% FC conditions in the LSL genotype (Table 1). Although relative

Table 1 Plant water status of tomato non-long shelf-life (nLSL) and long shelf-life (LSL) genotypes subjected to different conditions (control [CL], short-term water deficit stress at 40% FC [ST 40% FC], short-term water deficit stress at 30% FC [ST 30% FC], and short-term water deficit stress at 30% FC followed by recovery [ST 30% FC-Rec]). Mean values ± SE are shown for pre-dawn leaf water potential (Ψ_{pd}), midday leaf water potential (Ψ_{md}), and leaf relative water content (*RWC*). *RWC* was calculated in the same leaves in which Ψ_{md} was measured. Genotype (G) and treatment (T) effects were quantified by two-way ANOVA and differences between groups were analysed by LSD test. Different superscript letters indicate significant differences. $n = 5$ in all cases

Genotype and treatment	Ψ_{pd} (MPa)	Ψ_{md} (MPa)	*RWC* (%)
nLSL, CL	-0.24 ± 0.01^{a}	-0.40 ± 0.01^{a}	86.51 ± 0.05^{ab}
nLSL, ST 40% FC	-0.43 ± 0.02^{a}	-0.96 ± 0.03^{b}	82.07 ± 2.63^{ab}
nLSL, ST 30% FC	-0.89 ± 0.19^{b}	-1.34 ± 0.22^{c}	57.37 ± 5.12^{d}
nLSL, ST 30% FC-Rec	-0.32 ± 0.00^{a}	-0.43 ± 0.01^{a}	84.24 ± 1.20^{ab}
LSL, CL	-0.31 ± 0.03^{a}	-0.42 ± 0.02^{a}	88.33 ± 0.32^{a}
LSL, ST 40% FC	-0.42 ± 0.02^{a}	-0.54 ± 0.05^{a}	80.48 ± 2.01^{b}
LSL, ST 30% FC	-1.05 ± 0.09^{b}	-1.30 ± 0.05^{c}	70.22 ± 2.86^{c}
LSL, ST 30% FC-Rec	-0.26 ± 0.02^{a}	-0.43 ± 0.02^{a}	84.36 ± 1.73^{ab}
G	0.628	0.045	0.046
T	<0.001	<0.001	<0.001
G × T	0.588	0.071	0.040

water content (*RWC*) reductions were only significant under ST 30% FC conditions in the nLSL genotype, *RWC* was progressively reduced during water deficit stress treatments in the LSL genotype (Table 1). Remarkably, the reduction in *RWC* under ST 30% FC conditions was much larger in the nLSL genotype than in the LSL genotype (Table 1). In all cases, both genotypes restored previous parameters to CL values after ST 30% FC-Rec (Table 1).

Pressure–volume curves

In both genotypes, the decrease in leaf water potential at turgor loss point (Ψ_{tlp}) was specifically attributed to treatment effects ($P < 0.001$), achieving the lowest values under ST 30% FC conditions (Figure 1a). Whereas recovery almost restored Ψ_{tlp} to CL levels in the LSL genotype, it remained significantly lower in the nLSL genotype (−0.62 ± 0.02 and −0.53 ± 0.03 MPa, respectively; Figure 1a). *RWC* at turgor loss point (RWC_{tlp}) gradually increased after the application of water shortage treatments, being restored to CL in both genotypes upon recovery (Figure 1b). Note that despite the previously mentioned difference in *RWC* in both genotypes under ST 30% FC, both were below the wilting point according to RWC_{tlp} values (Table 1, Figure 1b). Although the pattern for the leaf osmotic potential at full turgor (π_o) resembled that of Ψ_{tlp}, both genotypes achieved similar values under ST 30% FC-Rec conditions, remaining significantly lower than under CL only in the nLSL genotype (Figure 1c). A significant treatment effect was detected

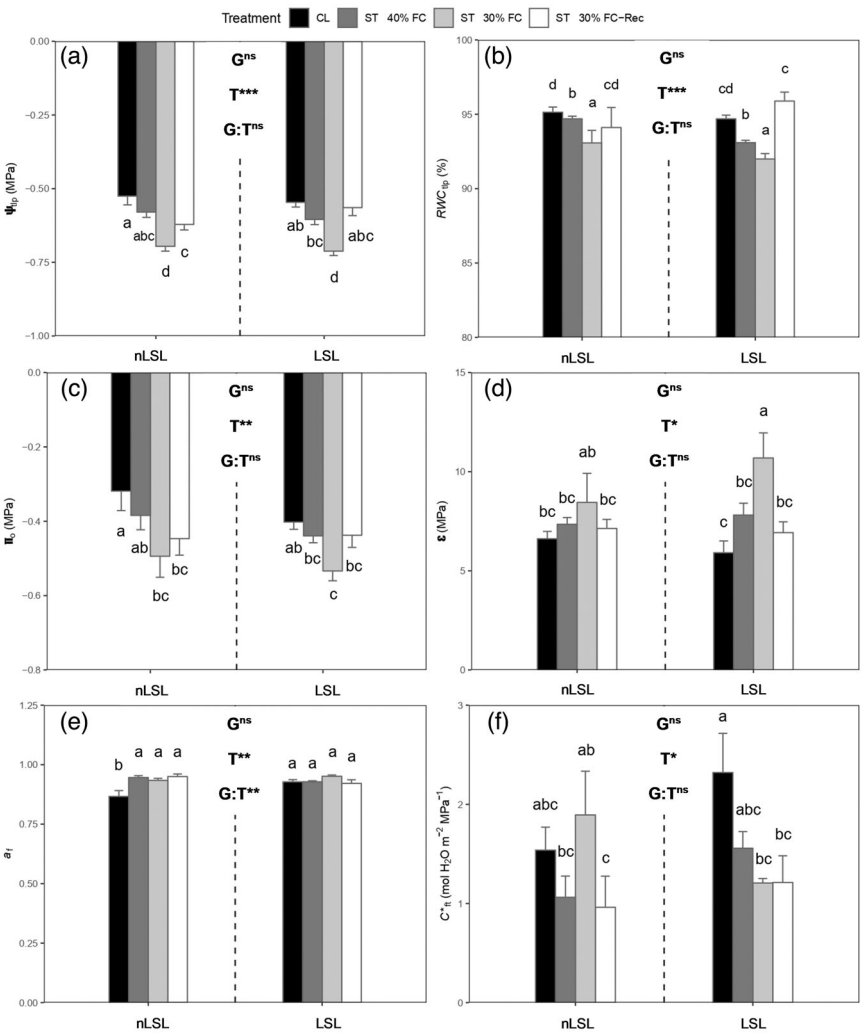

Figure 1. Leaf water relations of tomato non-long shelf-life (nLSL) and long shelf-life (LSL) genotypes subjected to different conditions (control [CL], short-term water deficit stress at 40% FC [ST 40% FC], short-term water deficit stress at 30% FC [ST 30% FC], and short-term water deficit stress at 30% FC followed by recovery [ST 30% FC-Rec]). (a) Water potential at turgor loss point (Ψ_{tlp}). (b) Relative water content at turgor loss point (RWC_{tlp}). (c) Osmotic potential at full turgor (π_o). (d) Bulk modulus of elasticity (ε). (e) Apoplastic water fraction (a_f). (f) Leaf area-specific capacitance at full turgor (C^*_{ft}). Genotype (G) and treatment (T) effects were quantified by two-way ANOVA and differences between groups were analysed by LSD test. Different superscript letters indicate significant differences. ***$P < 0.001$; **$P < 0.01$; *$P < 0.05$; ns, $P > 0.05$. Values are presented as means ± SE ($n = 5$).

for ε (P = 0.01). In this sense, ST 30% FC treatment increased leaf rigidity in the nLSL and LSL genotypes by 28 and 81%, respectively, as compared to CL (Figure 1d). In both cases, recovery restored ε to CL levels (Figure 1d). The nLSL genotype significantly increased the apoplastic water fraction (a_f) under all tested conditions in comparison to CL, while it was similarly maintained across all treatments in the LSL genotype (Figure 1e). A significant decrease in leaf area-specific capacitance at full turgor (C^*_{ft}) from 2.32 ± 0.40 to 1.21 ± 0.05 mol H_2O m^{-2} MPa^{-1} was observed in the LSL genotype under ST 30% FC conditions in comparison to CL, remaining similar to ST 30% FC levels upon recovery (Figure 1f). However, in the nLSL genotype, C^*_{ft} was reduced upon recovery as compared with ST 30% FC (Figure 1f).

Photosynthetic characterisation

The highest A_N value was found in the LSL genotype under CL conditions (20.23 ± 0.17 μmol CO_2 m^{-2} sec^{-1}), followed by the nLSL genotype under the same conditions (17.64 ± 0.86 μmol m^{-2} sec^{-1}; Figure 2a). ST 40% FC conditions decreased A_N by approximately 67 and 60% in nLSL and LSL genotypes, respectively, in comparison to CL (Figure 2a). Nonetheless, both genotypes reached similar A_N values under ST 30% FC (1.18 ± 0.09 and 1.61 ± 0.21 μmol CO_2 m^{-2} sec^{-1} for nLSL and LSL, respectively) and upon

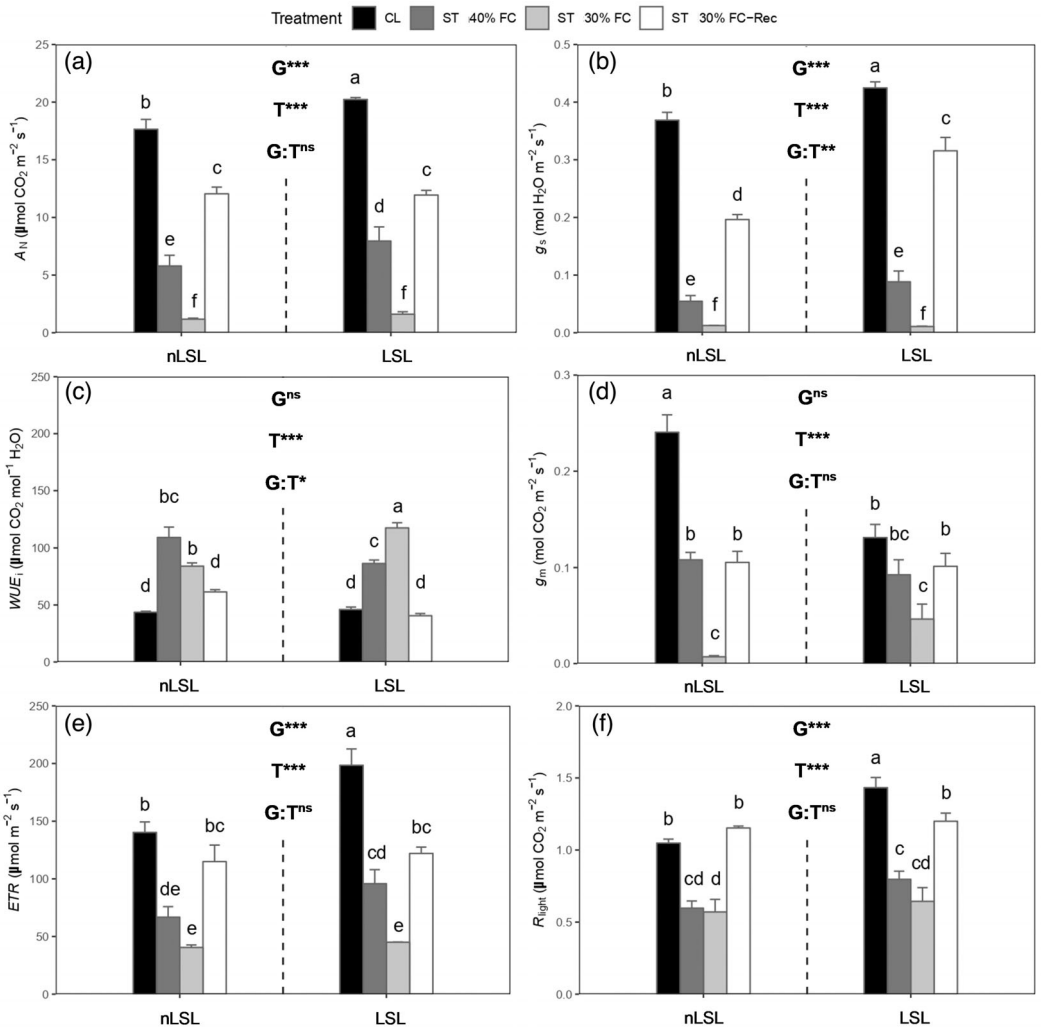

Figure 2. Photosynthetic characterisation of tomato non-long shelf-life (nLSL) and long shelf-life (LSL) genotypes subjected to different conditions (control [CL], short-term water deficit stress at 40% FC [ST 40% FC], short-term water deficit stress at 30% FC [ST 30% FC], and short-term water deficit stress at 30% FC followed by recovery [ST 30% FC-Rec]). (a) Net CO_2 assimilation (A_N). (b) Stomatal conductance (g_s). (c) Intrinsic water use efficiency (WUE_i). (d) Mesophyll conductance (g_m). (e) Electron transport rate (ETR). (f) Light respiration (R_{light}). Genotype (G) and treatment (T) effects were quantified by two-way ANOVA and differences between groups were analysed by LSD test. Different superscript letters indicate significant differences. ***P < 0.001; **P < 0.01; *P < 0.05; ns, P > 0.05. Values are presented as means ± SE (n = 5).

recovery, remaining significantly lower than under CL (Figure 2a). Apart from significant genotype and treatment effects ($P < 0.001$), a significant difference in the interaction term was also reported considering g_s ($P = 0.002$). Both genotypes achieved similar g_s values under ST 40% FC and ST 30% FC conditions, the latter representing a 97% reduction compared to CL levels (Figure 2b). Even though g_s did not reach CL values under ST 30% FC-Rec, the LSL genotype exhibited larger g_s values than the nLSL genotype under this condition (0.30 ± 0.02 and 0.19 ± 0.01 mol H_2O m^{-2} sec^{-1}; Figure 2b). Nonetheless, significant treatment and interaction term effects ($P < 0.001$ and $P = 0.011$, respectively) were only detected for WUE_i. Although both genotypes presented similar WUE_i values under CL conditions, it was progressively enhanced during the application of water shortage treatments, the LSL genotype reaching the largest value under ST 30% FC (191.96 ± 26.11 μmol CO_2 mol^{-1} H_2O; Figure 2c). Both genotypes restored WUE_i to CL levels upon recovery (Figure 2c). The nLSL genotype presented the highest g_m values under CL (0.25 ± 0.02 mol CO_2 m^{-2} sec^{-1}), which were almost 2-fold higher than those of the LSL genotype under the same condition (Figure 2d). Also, under ST 40% FC and ST 30% FC conditions, the nLSL genotype showed 56 and 96% reductions in g_m compared to CL levels, respectively (Figure 2d). However, in the LSL genotype, g_m reductions were only found under ST 30% FC (Figure 2d). While ST 30% FC-Rec restored g_m to CL levels in the LSL genotype, it remained similar to ST 40% FC levels in the nLSL genotype (Figure 2d). The highest electron transport rate (*ETR*) values were detected in the LSL genotype under CL (198.50 ± 14.14 μmol m^{-2} sec^{-1}), followed by the nLSL genotype under the same conditions (140.27 ± 9.07 μmol m^{-2} sec^{-1}; Figure 2e). Nonetheless, water deficit stress treatments significantly reduced *ETR* in both genotypes, reaching the lowest values under ST 30% FC (40.40 ± 2.17 and 45.05 ± 0.18 μmol m^{-2} sec^{-1} for nLSL and LSL, respectively; Figure 2e). Although recovery almost restored *ETR* to CL levels in the nLSL genotype, declines of around 40% were detected in the LSL genotype (Figure 2e). While the LSL genotype presented the highest light respiration (R_{light}) value under CL conditions (1.43 ± 0.07 μmol CO_2 m^{-2} sec^{-1}), it decreased due to water shortage treatments in both genotypes, reaching the lowest value in the nLSL genotype under ST 30% FC (0.71 ± 0.15 μmol CO_2 m^{-2} sec^{-1}; Figure 2f). Recovery restored R_{light} to CL levels in the nLSL genotype, but it remained significantly lower in the LSL genotype (Figure 2f).

Photosynthesis limitation analysis results are presented in Table 2. Under CL conditions, biochemical limitation (l_b) was the main *absolute* limiting factor in photosynthesis in both genotypes. Whereas l_b and stomatal limitation (l_s) similarly co-limited photosynthesis in both genotypes under ST 40% FC, l_s mainly limited A_N under ST 30% FC. Upon recovery, photosynthesis was mainly limited by l_b in both genotypes. Concerning *relative* contributions to limitations to d*A*/*A*, stomatal limitation (*SL*) mainly limited A_N under ST 40% FC and ST 30% FC conditions in both genotypes. However, under ST 30% FC-Rec, A_N was similarly co-limited by *SL*, mesophyll limitation (*ML*), and biochemical limitation (*BL*) in the nLSL genotype, while it was mostly limited by *BL* in the LSL genotype.

Cell wall composition characterisation

Differences in leaf cell wall composition were mainly attributed to genotype effects (Table 3). The highest alcohol-insoluble residue (AIR) amount was detected in the LSL genotype, whereas the lowest amounts were found in the nLSL genotype (Table 3). The nLSL genotype presented higher cellulose concentrations than the LSL genotype (Table 3). Nonetheless, slightly higher amounts of hemicelluloses were detected in the LSL genotype than in the nLSL

Table 2 Photosynthesis limitations analysis of tomato non-long shelf-life (nLSL) and long shelf-life (LSL) genotypes subjected to different conditions (control [CL], short-term water deficit stress at 40% FC [ST 40% FC], short-term water deficit stress at 30% FC [ST 30% FC], and short-term water deficit stress at 30% FC followed by recovery [ST 30% FC-Rec]). Mean values ± SE are shown for *absolute* stomatal (l_s), mesophyll (l_m), and biochemical (l_b) limitations as well as for *relative* stomatal (*SL*), mesophyll (*ML*), and biochemical (*BL*) contributions to d*A*/*A* according to Grassi and Magnani (2005). Genotype (G) and treatment (T) effects were quantified by two-way ANOVA. $n = 5$ in all cases

Genotype and treatment	l_s	l_m	l_b	*SL* (%)	*ML* (%)	*BL* (%)
nLSL, CL	0.20 ± 0.01	0.19 ± 0.02	0.61 ± 0.03			
nLSL, ST 40% FC	0.46 ± 0.06	0.12 ± 0.03	0.42 ± 0.03	34.04 ± 2.41	5.96 ± 0.05	22.30 ± 3.89
nLSL, ST 30% FC	0.60 ± 0.07	0.15 ± 0.08	0.24 ± 0.02	58.90 ± 6.93	21.47 ± 5.78	17.77 ± 1.61
nLSL, ST 30% FC-Rec	0.31 ± 0.04	0.23 ± 0.05	0.46 ± 0.04	13.23 ± 0.89	11.44 ± 4.79	12.59 ± 3.11
LSL, CL	0.20 ± 0.01	0.34 ± 0.05	0.45 ± 0.05			
LSL, ST 40% FC	0.42 ± 0.04	0.21 ± 0.04	0.37 ± 0.01	33.95 ± 5.09	8.81 ± 2.93	18.93 ± 2.13
LSL, ST 30% FC	0.71 ± 0.08	0.05 ± 0.02	0.24 ± 0.02	68.39 ± 8.35	0.80 ± 0.00	19.48 ± 2.17
LSL, ST 30% FC-Rec	0.18 ± 0.01	0.34 ± 0.03	0.48 ± 0.03	4.79 ± 1.17	8.85 ± 4.73	18.59 ± 1.86
G	0.253	0.012	0.131	0.380	0.212	0.531
T	<0.001	0.024	<0.001	<0.001	0.348	0.161
G × T	0.095	0.013	0.039	0.113	0.226	0.239

genotype (Table 3). Finally, pectins were the only cell wall component presenting significant differences due to genotype and treatment effects as well as in the interaction term (Table 3). Whereas a tendency to increase pectins content was found in both genotypes when applying water deprivation, larger amounts of pectins were observed in the nLSL genotype (Table 3). Upon recovery, pectins levels were similar to those in water shortage conditions in the nLSL genotype, while they remained significantly higher than under CL conditions in the LSL genotype (Table 3).

Foliar structure and anatomical characterisation

Concerning foliar structure, significant differences in LMA were only reported in the nLSL genotype under CL and in the nLSL genotype under ST 30% FC (Table 4). However, no significant differences in leaf density (LD) were found (Table 4). Regarding anatomical characterisation from semi-fine cross-sections, both genotypes presented the largest T_{leaf} values under CL conditions, being slightly higher in the LSL genotype (238.03 ± 3.77 μm; Table 4). Although T_{leaf} was gradually reduced in the nLSL genotype upon water shortage application, the lowest value in the LSL genotype was observed under ST 40% FC conditions (187.66 ± 5.27 μm; Table 4). Upon recovery, T_{leaf} remained 20 and 12% lower than under CL in the nLSL and LSL genotypes, respectively (Table 4). A similar pattern was found for T_{mes} (Table 4). Finally, only a significant genotype effect was detected for the fraction of mesophyll intercellular air space (f_{ias}) since the nLSL genotype presented higher porosity than the LSL genotype (Table 4). In relation to the analysis of ultra-fine cross-sections, water deprivation treatments and ST 30% FC-Rec caused significant decreases in chloroplast thickness (T_{chl}) and chloroplast length (L_{chl}) as compared to CL conditions in both genotypes (Table 5). Similarly, water deficit stress reduced the mesophyll and chloroplast surface area exposed to intercellular air space per leaf area (S_m/S and S_c/S, respectively) in both genotypes, which were restored to CL levels upon recovery in the LSL genotype (Table 5). Instead, ST 30% FC-Rec reduced S_m/S and S_c/S values even further than water shortage treatments in the nLSL genotype (Table 5). Both genotypes exhibited the highest S_c/S_m ratio under CL conditions (Table 5). Although the nLSL genotype achieved the lowest S_c/S_m ratio under ST 40% FC, it was gradually reduced during water deprivation in the LSL genotype (Table 5). Upon recovery, the S_c/S_m ratio was restored to CL levels in the nLSL genotype, while it remained significantly lower in the LSL genotype (Table 5). Changes in T_{cw} were exclusively attributed to treatment effects (Table 5). Even though water shortage treatments decreased T_{cw} in the LSL genotype, it was maintained at CL levels in the nLSL genotype (Table 5). Nonetheless, whereas T_{cw} was restored to CL levels upon recovery in the LSL genotype, T_{cw} increased in the nLSL genotype under the same conditions (Table 5). Finally, statistical analysis of g_m based on anatomical measurements revealed that only the treatment effect was significant since g_m decreased under water deficit stress as well as upon recovery in comparison to CL in both genotypes (Table S2).

Principal component analysis

A principal component analysis (PCA) was performed, in which two principal components (PCs) accounted for 71.3% of the total variation (Figure 3). PC1 (accounting for 47.4% of total variation) was mostly represented by gas exchange (A_N, g_s, and *ETR*) and anatomical parameters (S_c/S and T_{chl}), while cell wall components and foliar traits (i.e., LMA and LD) were mostly observed in PC2 (accounting for 23.9% of total variation). Interestingly, the representation of the tested genotypes and experimental conditions

Table 3 Leaf cell wall composition of tomato non-long shelf-life (nLSL) and long shelf-life (LSL) genotypes subjected to different conditions (control [CL], short-term water deficit stress at 40% FC [ST 40% FC], short-term water deficit stress at 30% FC [ST 30% FC], and short-term water deficit stress at 30% FC followed by recovery [ST 30% FC-Rec]). Mean values ± SE are shown for alcohol-insoluble residue (AIR), cellulose, hemicelluloses, and pectins contents. Genotype (G) and treatment (T) effects were quantified by two-way ANOVA and differences between groups were analysed by LSD test. Different superscript letters indicate significant differences. $n = 5$ in all cases

Genotype and treatment	AIR (g g^{-1} DW)	Cellulose (mg g^{-1} AIR)	Hemicelluloses (mg g^{-1} AIR)	Pectins (mg g^{-1} AIR)
nLSL, CL	0.08 ± 0.01^{c}	120.39 ± 9.00^{ab}	283.43 ± 7.81^{c}	41.01 ± 3.16^{bc}
nLSL, ST 40% FC	0.09 ± 0.01^{bc}	108.89 ± 4.58^{abc}	346.64 ± 45.35^{abc}	68.28 ± 2.78^{a}
nLSL, ST 30% FC	0.07 ± 0.01^{c}	109.83 ± 3.85^{abc}	377.42 ± 61.20^{abc}	62.22 ± 3.75^{a}
nLSL, ST 30% FC-Rec	0.07 ± 0.01^{c}	130.42 ± 12.00^{a}	306.65 ± 31.23^{bc}	64.57 ± 2.26^{a}
LSL, CL	0.12 ± 0.01^{a}	80.96 ± 6.37^{d}	456.61 ± 60.49^{a}	27.87 ± 1.09^{d}
LSL, ST 40% FC	0.10 ± 0.01^{ab}	101.29 ± 15.63^{bcd}	402.25 ± 30.99^{abc}	33.75 ± 1.89^{cd}
LSL, ST 30% FC	0.08 ± 0.01^{abc}	92.28 ± 10.09^{cd}	443.10 ± 36.28^{ab}	44.18 ± 4.56^{b}
LSL, ST 30% FC-Rec	0.09 ± 0.01^{abc}	102.72 ± 5.76^{bcd}	415.12 ± 56.31^{ab}	39.04 ± 1.02^{bc}
G	<0.001	<0.001	<0.001	<0.001
T	0.076	0.240	0.706	<0.001
G × T	0.820	0.335	0.571	0.003

Table 4 Leaf structural and anatomical characterisation from semi-fine cross-sections of tomato non-long shelf-life (nLSL) and long shelf-life (LSL) genotypes subjected to different conditions (control [CL], short-term water deficit stress at 40% FC [ST 40% FC], short-term water deficit stress at 30% FC [ST 30% FC], and short-term water deficit stress at 30% FC followed by recovery [ST 30% FC-Rec]). Mean values ± SE are shown for leaf mass per area (LMA), leaf density (LD), leaf thickness (T_{leaf}), mesophyll thickness (T_{mes}), and fraction of mesophyll intercellular air space (f_{ias}). Genotype (G) and treatment (T) effects were quantified by two-way ANOVA and differences between groups were analysed by LSD test. Different superscript letters indicate significant differences. $n = 5$ in all cases

Genotype and treatment	LMA (g m^{-2})	LD (g cm^{-3})	T_{leaf} (μm)	T_{mes} (μm)	f_{ias} (%)
nLSL, CL	47.53 ± 5.12^{b}	0.11 ± 0.01^{a}	222.01 ± 17.76^{ab}	173.85 ± 15.88^{ab}	29.04 ± 2.53^{abc}
nLSL, ST 40% FC	53.57 ± 6.54^{ab}	0.13 ± 0.02^{a}	193.21 ± 5.11^{cd}	147.15 ± 0.57^{bcd}	34.04 ± 2.50^{a}
nLSL, ST 30% FC	60.34 ± 1.94^{ab}	0.16 ± 0.01^{a}	163.12 ± 11.04^{e}	118.78 ± 9.26^{e}	32.84 ± 2.21^{ab}
nLSL, ST 30% FC-Rec	54.84 ± 9.20^{ab}	0.15 ± 0.03^{a}	179.04 ± 7.70^{de}	138.79 ± 3.35^{de}	34.68 ± 3.25^{a}
LSL, CL	60.80 ± 5.54^{ab}	0.14 ± 0.01^{a}	238.03 ± 3.77^{a}	193.47 ± 2.22^{a}	24.10 ± 1.21^{c}
LSL, ST 40% FC	64.97 ± 9.13^{ab}	0.15 ± 0.02^{a}	187.66 ± 5.27^{cde}	145.85 ± 2.77^{cd}	25.00 ± 3.39^{c}
LSL, ST 30% FC	71.05 ± 2.73^{a}	0.17 ± 0.01^{a}	212.77 ± 7.71^{abc}	165.12 ± 8.45^{bc}	26.95 ± 2.73^{bc}
LSL, ST 30% FC-Rec	59.51 ± 3.65^{ab}	0.17 ± 0.00^{a}	207.71 ± 9.02^{bc}	162.02 ± 5.47^{bcd}	23.12 ± 0.86^{c}
G	0.030	0.159	0.003	0.002	<0.001
T	0.252	0.079	<0.001	<0.001	0.514
G × T	0.890	0.973	0.060	0.093	0.532

Table 5 Leaf anatomical characterisation from ultra-fine cross-sections of tomato non-long shelf-life (nLSL) and long shelf-life (LSL) genotypes subjected to different conditions (control [CL], short-term water deficit stress at 40% FC [ST 40% FC], short-term water deficit stress at 30% FC [ST 30% FC], and short-term water deficit stress at 30% FC followed by recovery [ST 30% FC-Rec]). Mean values ± SE are shown for chloroplast thickness (T_{chl}), chloroplast length (L_{chl}), mesophyll and chloroplast surface area exposed to intercellular air space per leaf area (S_m/S and S_c/S, respectively), the S_c/S_m ratio, and cell wall thickness (T_{cw}). Genotype (G) and treatment (T) effects were quantified by two-way ANOVA and differences between groups were analysed by LSD test. Different superscript letters indicate significant differences. $n = 5$ in all cases

Genotype and treatment	T_{chl} (μm)	L_{chl} (μm)	S_m/S (m^2 m^{-2})	S_c/S (m^2 m^{-2})	S_c/S_m	T_{cw} (μm)
nLSL, CL	5.53 ± 0.05^{a}	2.91 ± 0.15^{ab}	17.86 ± 0.74^{a}	16.10 ± 0.91^{a}	0.90 ± 0.02^{a}	0.11 ± 0.00^{b}
nLSL, ST 40% FC	4.63 ± 0.05^{b}	2.72 ± 0.14^{ab}	15.98 ± 0.25^{abc}	$12. 30 \pm 0.18^{bcd}$	0.79 ± 0.02^{bc}	0.11 ± 0.01^{b}
nLSL, ST 30% FC	4.52 ± 0.15^{b}	2.58 ± 0.24^{b}	14.31 ± 0.87^{bc}	12.47 ± 1.01^{bcd}	0.86 ± 0.02^{ab}	0.11 ± 0.01^{b}
nLSL, ST 30% FC-Rec	4.74 ± 0.13^{b}	2.27 ± 0.13^{b}	13.72 ± 1.57^{c}	10.23 ± 1.11^{d}	0.84 ± 0.02^{abc}	0.13 ± 0.00^{a}
LSL, CL	5.95 ± 0.27^{a}	3.23 ± 0.28^{a}	17.28 ± 1.85^{ab}	15.29 ± 1.54^{ab}	0.88 ± 0.03^{a}	0.13 ± 0.01^{a}
LSL, ST 40% FC	4.75 ± 0.25^{b}	2.68 ± 0.31^{ab}	15.96 ± 0.33^{abc}	12.58 ± 0.77^{bcd}	0.79 ± 0.05^{bc}	0.12 ± 0.01^{ab}
LSL, ST 30% FC	4.62 ± 0.20^{b}	2.64 ± 0.12^{ab}	15.10 ± 0.10^{abc}	11.16 ± 0.40^{cd}	0.75 ± 0.01^{c}	0.10 ± 0.02^{b}
LSL, ST 30% FC-Rec	4.87 ± 0.33^{b}	2.38 ± 0.28^{b}	15.63 ± 0.96^{abc}	13.31 ± 0.95^{abc}	0.78 ± 0.04^{bc}	0.12 ± 0.00^{ab}
G	0.112	0.394	0.406	0.470	0.044	0.149
T	<0.001	0.016	0.042	0.001	0.005	0.047
G × T	0.863	0.886	0.710	0.158	0.237	0.150

grouped differently, indicating that each treatment elicited distinct responses in different genotypes.

Relationships between parameters

Correlations between all tested parameters for each genotype are presented in Tables S3 and S4. No significant correlations were detected between photosynthetic, leaf water relations, sub-cellular anatomic, and cell wall composition parameters in the nLSL genotype. However, significant relationships were observed for the LSL genotype (Figures 4 and 5). Hence, while g_m was positively correlated with the (Cellulose + Hemicelluloses)/Pectins ratio ($R^2 = 0.99$, $P < 0.01$, Figure 4a), a negative relationship with ε was found ($R^2 = 0.92$, $P = 0.03$, Figure 4b). In turn, ε and the (Cellulose + Hemicelluloses)/Pectins ratio were negatively correlated ($R^2 = 0.95$, $P = 0.02$, Figure 4c). Positive correlations between g_m and S_c/S and T_{cw} were detected ($R^2 = 0.98$, $P < 0.01$, Figure 5a and $R^2 = 0.98$, $P < 0.01$, Figure 5b, respectively). Although ε and S_c/S were not significantly correlated (Figure 5c), a negative relationship between ε and T_{cw} was observed ($R^2 = 0.95$, $P = 0.02$, Figure 5d). Finally, a positive relationship between S_c/S and the (Cellulose + Hemicelluloses)/Pectins ratio was found ($R^2 = 0.94$, $P = 0.02$, Figure 5e), as well as for T_{cw} and the (Cellulose + Hemicelluloses)/Pectins ratio ($R^2 = 0.99$, $P < 0.01$, Figure 5f). Regarding those significant correlations exclusively detected in the nLSL genotype, g_m was linked negatively with LMA ($R^2 = 0.95$, $P = 0.02$, Figure 6a).

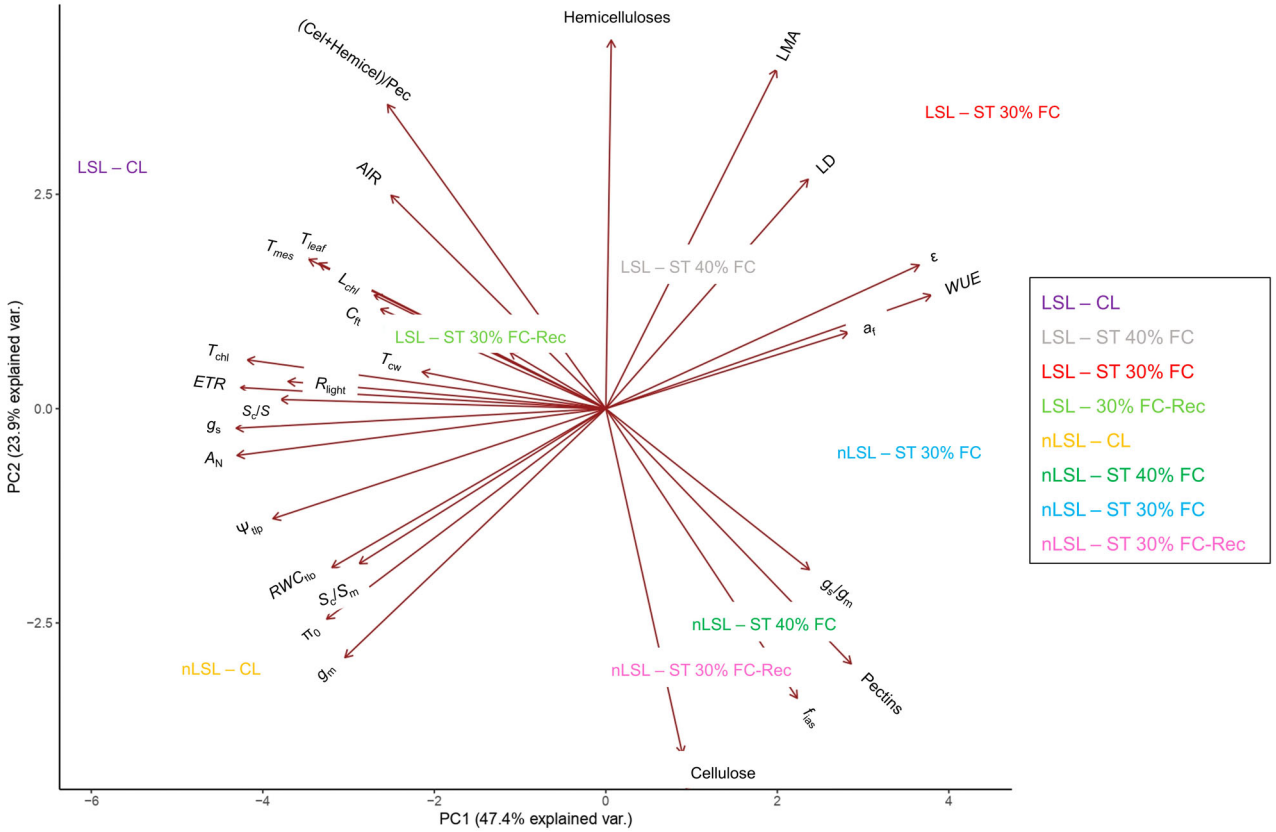

Figure 3. Principal component analysis (PCA) of gas exchange, cell wall, pressure–volume, and anatomical parameters of both genotypes subjected to different treatments. The same abbreviations as in Figures and Tables are used except for the (Cellulose + Hemicelluloses)/Pectins ratio, which is shown as '(Cel + Hemicel)/Pectin'. Axes represent the two principal components (PCs), which together explain 71.3% of the total variance.

However, positive relationships between g_m and T_{leaf} and T_{mes} were observed (R^2 = 0.95, P = 0.02, Figure 5c and R^2 = 0.99, P < 0.01, Figure 6d, respectively).

DISCUSSION

Water shortage is recognised as one of the most important abiotic stresses affecting plants' physiological performance (Chaves et al., 2009; Flexas et al., 2004; Nadal & Flexas, 2019). In fact, changes in leaf water relations – particularly osmotic and elastic adjustments – usually occur under water deficit stress (Abrams, 1990; Galmés et al., 2011; Kubiske & Abrams, 1991; Lo Gullo & Salleo, 1988; Nadal et al., 2020; Turner, 2018; Xiong & Nadal, 2020). In our study, we detected declines in π_o in both genotypes once subjected to water deprivation (in particular, under ST 30% FC), as commonly described (Abrams, 1990; Bartlett et al., 2012; Kubiske & Abrams, 1991; Lo Gullo & Salleo, 1988; Nadal et al., 2020; Turner, 2018). Although both genotypes presented similar reductions in π_o under water shortage conditions, elastic modifications were of higher relevance in the LSL genotype (Figure 1). In fact, ε adjustments occurring under water deficit stress are variable (see, for instance, Sobrado & Turner, 1983; Lo Gullo & Salleo, 1988; Nadal et al., 2020; Roig-Oliver, Bresta, Nadal, et al., 2020; Roig-Oliver, Nadal, Bota, et al., 2020; Roig-Oliver, Nadal, Clemente-Moreno, et al., 2020; Roig-Oliver, Fullana-Pericàs, et al., 2021), suggesting that they could be species-dependent. Furthermore, Galmés et al. (2011) reported genotype-dependent elastic adjustments testing well-watered and water-stressed nLSL and LSL tomato genotypes. While they showed that most of the analysed genotypes increased leaf rigidity (i.e., higher ε) during water deprivation probably to avoid excessive water losses, ε was not modified in others. Hence, our results provide further evidence on the genotype-dependent elastic adjustments occurring in tomato genotypes (Figure 1).

Besides modifications in leaf water relations, the application of different water availability treatments also promoted distinct photosynthetic responses in the tested genotypes (Figure 2). Under CL conditions, the LSL genotype achieved larger A_N values than the nLSL genotype because of increases in both g_s and *ETR* even when presenting lower g_m. This photosynthetic behaviour for both genotypes was linked to a photosynthesis limitation mainly attributed to l_b (Table 2). In fact, Nadal and Flexas (2019) highlighted that increasing biochemical

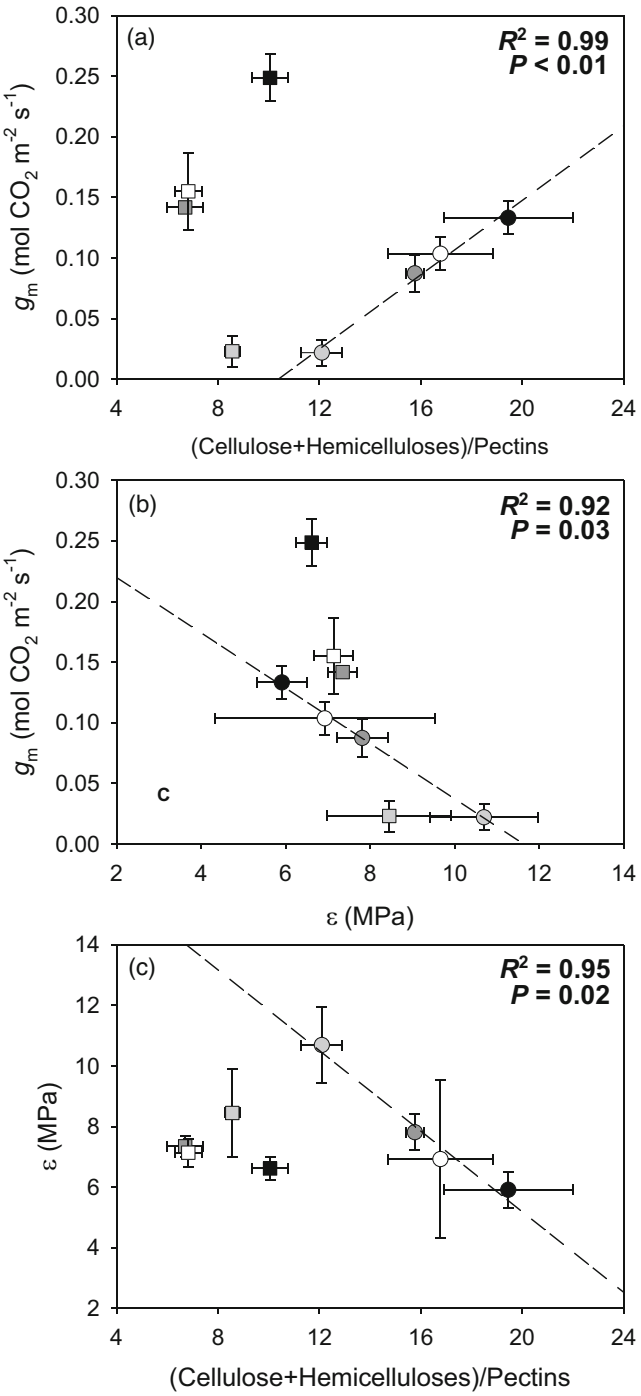

Figure 4. (a) Relationship between mesophyll conductance (g_m) and the (Cellulose + Hemicelluloses)/Pectins ratio. (b) Relationship between mesophyll conductance (g_m) and the bulk modulus of elasticity (ε). (c) Relationship between the bulk modulus of elasticity (ε) and the (Cellulose + Hemicelluloses)/Pectins ratio. When significant, regression lines, regression square coefficients, and significances are shown. Discontinuous and solid regression lines correspond to LSL and nLSL genotypes, respectively. Whereas nLSL genotype values are represented by squares, LSL genotype values are represented by circles. Black, dark grey, grey, and white correspond to CL, ST 40% FC, ST 30% FC, and ST 30%-Rec treatments, respectively. $n = 5$ (means ± SE).

processes rather than only increasing g_m could significantly improve A_N in well-watered crops. Even though both genotypes reduced g_s to the same extent under ST 40% FC, the LSL genotype presented smaller reductions in *ETR* than the nLSL genotype. Also, the LSL genotype maintained g_m close to CL levels, whereas significant declines were observed in the nLSL genotype. These different photosynthetic modifications taking place in both genotypes

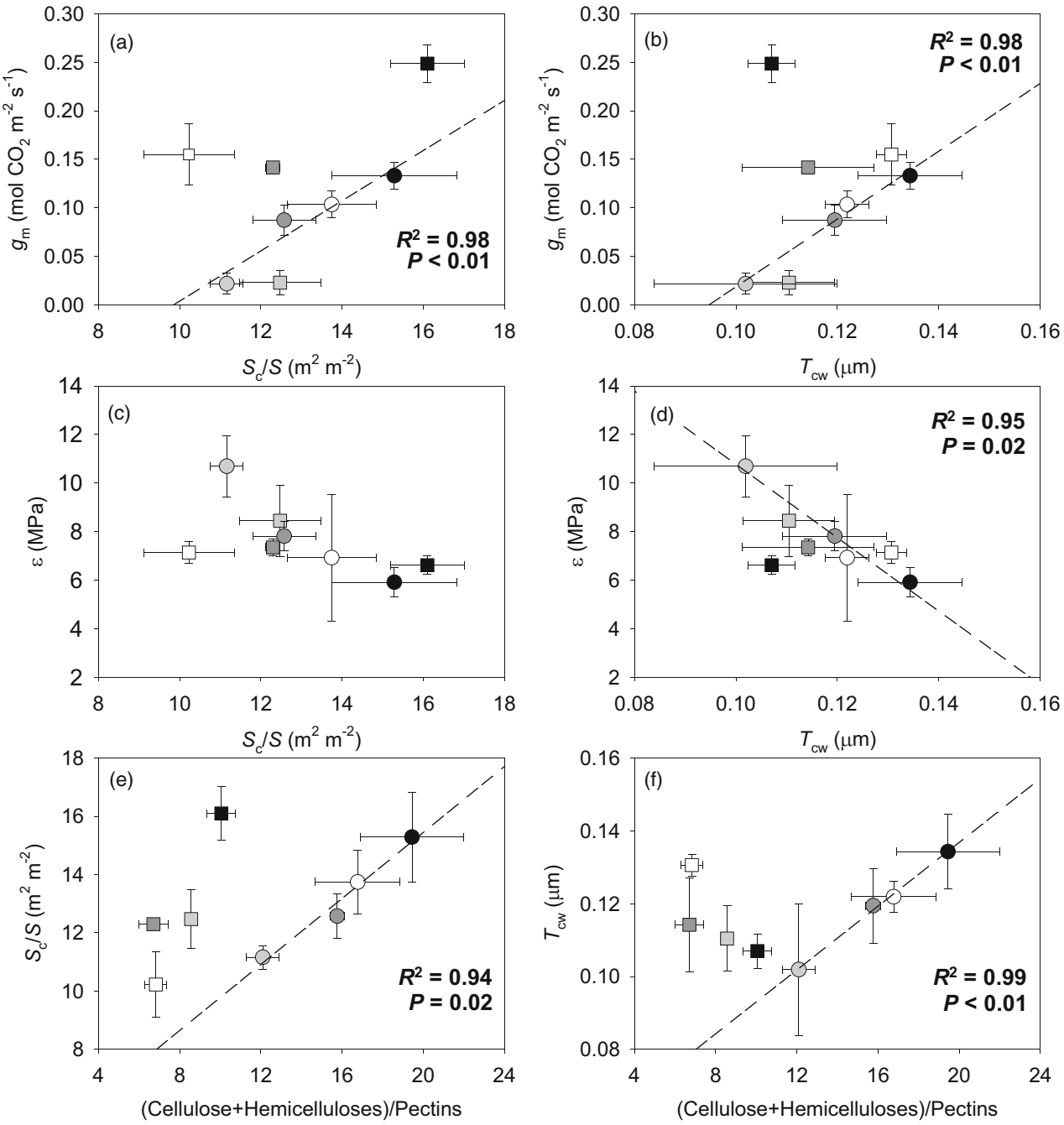

Figure 5. (a, b) Relationships between mesophyll conductance (g_m) and (a) chloroplast surface area exposed to intercellular air space per leaf area (S_c/S) and (b) cell wall thickness (T_{cw}). (c, d) Relationships between the bulk modulus of elasticity (ε) and (c) chloroplast surface area exposed to intercellular air space per leaf area (S_c/S) and (d) cell wall thickness (T_{cw}). (e, f) Relationships between the (Cellulose + Hemicelluloses)/Pectins ratio and (e) chloroplast surface area exposed to intercellular air space per leaf area (S_c/S) and (f) cell wall thickness (T_{cw}). When significant, regression lines, regression square coefficients, and significances are shown. Discontinuous and solid regression lines correspond to LSL and nLSL genotypes, respectively. Whereas nLSL genotype values are represented by squares, LSL genotype values are represented by circles. Black, dark grey, grey, and white correspond to CL, ST 40% FC, ST 30% FC, and ST 30%-Rec treatments, respectively. $n = 5$ (means ± SE).

resulted in the LSL genotype achieving larger A_N values than the nLSL genotype under ST 40% FC conditions. Overall, the distinct photosynthetic adjustments occurring in both genotypes allowed the LSL genotype to reach higher A_N values under CL and to increase WUE_i to a larger extent, being linked to less variable g_m across experimental conditions as compared to the nLSL genotype. Nonetheless, similar photosynthetic increases were

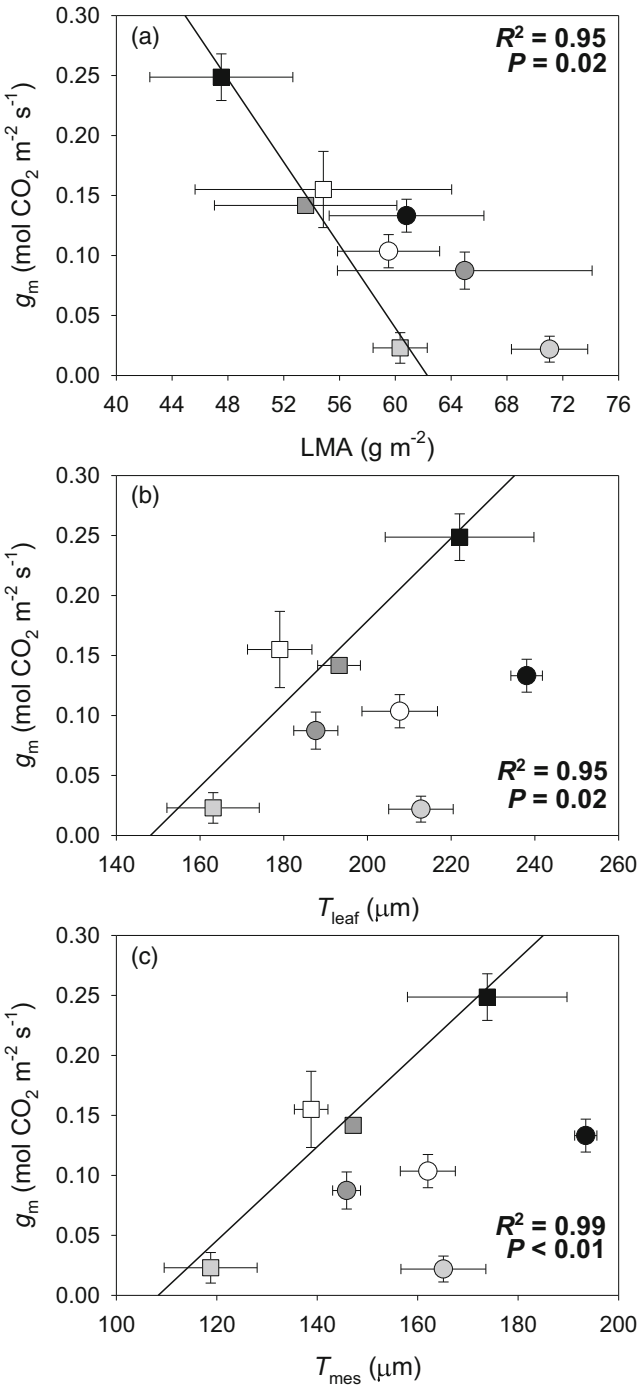

Figure 6. (a–c) Relationships between mesophyll conductance (g_m) and (a) leaf mass per area (LMA), (b) leaf thickness (T_{leaf}), and (c) mesophyll thickness (T_{mes}). When significant, regression lines, regression square coefficients, and significances are shown. Discontinuous and solid regression lines correspond to LSL and nLSL genotypes, respectively. Whereas nLSL genotype values are represented by squares, LSL genotype values are represented by circles. Black, dark grey, grey, and white correspond to CL, ST 40% FC, ST 30% FC, and ST 30%-Rec treatments, respectively. $n = 5$ (means ± SE).

observed in both genotypes after ST 30% FC-Rec, which were mostly driven by increases in g_s. However, full recovery of g_s and A_N was not achieved (Figure 2).

While it is often thought that modifications in the cell wall composition of mature leaves are of lesser magnitude than those occurring during leaf development and expansion (Cosgrove, 2018; Houston et al., 2016), recent studies have reported highly dynamic modifications from a compositional perspective (Roig-Oliver, Bresta, et al., 2021; Roig-Oliver, Bresta, Nadal, et al., 2020). In these studies,

active cell wall composition turnover was detected in sunflowers (*Helianthus annuus*) subjected to 2 days of recovery after the application of short- and long-term water deficit stresses (Roig-Oliver, Bresta, Nadal, et al., 2020). An extended experimental design of the previous experiment showed that pectins and hemicelluloses were significantly modified after only 5 and 24 h of rewatering, respectively, preceded by a long-term water deprivation (Roig-Oliver, Bresta, et al., 2021). Together with the results observed in other species, it has been proposed that changes in cell wall composition of mature leaves during abiotic stresses application could regulate g_m and/or ε adjustments in a species-dependent way (Clemente-Moreno et al., 2019; Roig-Oliver, Bresta, et al., 2021; Roig-Oliver, Fullana-Pericàs, et al., 2021; Roig-Oliver, Bresta, Nadal, et al., 2020; Roig-Oliver, Nadal, Bota, et al., 2020; Roig-Oliver, Nadal, Clemente-Moreno, et al., 2020). Interestingly, here we show that the role of the cell wall composition in determining these functional traits differs even between different genotypes of the same species. Particularly, these cell wall-mediated effects on distinct plant functional traits were mainly attributed to changes in relative pectins proportion (Figure 4). In fact, pectins are thought to be of crucial relevance in the maintenance of an appropriate degree of cell wall hydration during water shortage (Rui & Dinneny, 2019; Tenhaken, 2015). Moreover, modifications in their amounts are probably accompanied by changes in their physicochemical structure due to alterations in the enzymatic performance of pectin-remodelling enzymes, whose overexpression/knockdown can disrupt signalling pathways, hence changing the status, dynamics, and organisation of the cell wall (Anderson & Kieber, 2020; Cosgrove, 2005; Park & Cosgrove, 2012; Tucker et al., 2018). Consequently, these modifications in cell wall architecture could potentially influence elasticity, thickness, and porosity, key traits affecting g_m (Flexas et al., 2021). Since we found that changes in the relative proportion of major cell wall components were significantly linked with ε, T_{cw}, and S_c/S in the LSL genotype (Figures 4c and 5e,f), it could be expected that these cell wall modifications may finally affect g_m, as shown in Figure 4(a). However, these previously mentioned relationships were non-significant in the nLSL genotype. Therefore, we cannot discard the possibility that other traits not studied here could be involved in g_m regulation, especially in this genotype. On the one hand, we suggest that changes in the concentrations of other cell wall components – for instance, cell wall-bound phenolics and/or lignins – could have influenced g_m regulation across experimental conditions, as shown in sunflowers subjected to contrasting water regimes (Roig-Oliver, Bresta, Nadal, et al., 2020). On the other hand, it could be possible that aquaporins or carbonic anhydrases may have influenced g_m, as reported by Pérez-Martín et al. (2014). In any of these cases, further studies would be required to analyse how these traits could potentially affect g_m in both genotypes, especially in nLSL ones.

Besides the relevance of cell wall composition, sub-cellular anatomical traits – specifically T_{cw} and S_c/S – also determined g_m from a species-dependent perspective during acclimation to distinct environmental stresses (Galmés et al., 2013; Hanba et al., 2002; Tholen et al., 2008; Tosens et al., 2012). Here, we show that the correlations between g_m and S_c/S and T_{cw} differently occurred at genotype level (Figure 5a,b), as similarly happened with those between ε and S_c/S and T_{cw} (Figure 5c,d). Particularly, they were only significant for the LSL genotype, which increased g_m and reduced ε while enhancing T_{cw}, contradicting the hypothesis that thicker cell walls restrict CO_2 diffusion (Flexas & Carriquí, 2020; Gago et al., 2019) and result in more rigid leaves (Nadal et al., 2018; Peguero-Pina et al., 2017). However, we speculate that the LSL genotype could experience T_{cw} reductions during water deprivation that may have been accompanied by dynamic changes in cell wall composition – specifically increased pectins amounts – enabling these plants to partially maintain g_m. This may represent a case of fine anatomical–physiological plasticity that could allow for increased WUE_i. Instead, the nLSL genotype similarly maintained T_{cw} and cell wall composition across treatments, promoting strong g_m declines once subjected to water shortage, which could be attributed to changes in foliar traits and to supra-cellular anatomy, particularly an increase in LMA and reductions in T_{leaf} and T_{mes} (Figure 6). These results may suggest that the nLSL genotype adjusted g_m by supra-cellular adjustments and/or because of mesophyll collapse due to a very strong decrease in *RWC* (Table 1). Actually, the latter is more compatible with the fact that it seems a collapse more than a regulation in the sense that nLSL plants decreased photosynthesis as well as WUE_i.

In pot experiments like the present, heterogeneity is created among soil layers when applying water deficit treatments (Dodd, 2007; Saradadevi et al., 2015), for which the physiological behaviour observed here cannot be totally extrapolated to what could happen under field conditions. Nonetheless, our main aim in diversifying treatments was to create a source of variation to extend the axes of our correlations, allowing us to present strong correlations among parameters. The present study shows that the relationship between cell wall composition and physiological behaviour in plants subjected to distinct water regimes could be genotype-dependent within a single and thoroughly selected crop species. While the LSL genotype maintained g_m within a narrow range across experimental conditions probably due to elastic, sub-cellular anatomic, and cell wall composition adjustments, the nLSL genotype experienced large g_m variations that seemed to be linked to changes in foliar traits and in supra-cellular anatomical characteristics. Since both genotypes exhibited contrasting

responses for most of the analysed parameters (Figure 3), we suggest that cell wall composition modifications occurring in the LSL genotype might be crucial during their adaptation to drought environments and could sustain their productivity under the climate change scenario. Although non-significant relationships between g_m and cell wall components were detected in the nLSL genotype, we cannot rule out that lignins or cell wall-bound phenolics, as well as aquaporins or carbonic anhydrases, could influence g_m. However, even in this case, and considering our results, it appears that LSL plants achieved larger benefits – at least at the leaf level – from their regulation syndrome than nLSL ones. Thus, it will be crucial to perform a more in-depth analysis in a larger number of tomato LSL and nLSL genotypes subjected to more treatments in order to draw conclusive statements regarding the relevance of modifications in the cell wall composition influencing photosynthetic, biochemical, and anatomical traits.

EXPERIMENTAL PROCEDURES

Plant material selection and preparation

Tomato genotypes were selected based on their leaf morphology and growth type since these traits influence their physiological performance (Galmés et al., 2011). The 'Ailsa Craig' genotype was used as nLSL genotype, while a 'de Ramellet' genotype (accession UIB1-28 according to the University of the Balearic Islands seed bank code) was employed as LSL genotype. Seeds of the nLSL genotype were kindly provided by Dr Eva Domínguez (EELM-CSIC, Malaga) and seeds of the LSL genotype were obtained from the University of the Balearic Islands seed bank. Both genotypes presented indeterminate growth and the common divided tomato leaf morphology.

Following Fullana-Pericàs et al. (2019), an antiviral treatment was applied to all seeds before sowing. They were submerged in a 10% sodium triphosphate solution for 3 h and subsequently cleaned with distilled water. Then, seeds were submerged in a 30% commercial bleach solution for 1 h, washed again with distilled water, and air-dried at room temperature for 24 h. Seeds were kept in a hermetic container filled with silica gel for at least 24 h before being placed in an oven at 70°C for 24 h.

Growth conditions and experimental design

After the application of the antiviral treatment, seeds were sown individually in water-irrigated 3-L pots containing a substrate mixture of peat and perlite (3:1, v/v). All pots were placed in a growth chamber at 25°C receiving 300 μmol m^{-2} sec^{-1} photosynthetic photon flux density (PPFD) for 12 h, followed by 12 h of darkness. Pots were daily monitored to be watered to 100% FC by replacing evapo-transpired water, receiving Hoagland's solution 50% once a week. Twenty-eight days after sowing – when all plants presented at least three or four fully developed leaves – four treatments were established: (i) control (CL, i.e., without stress), (ii) short-term water deficit stress at 40% FC (ST 40% FC), (iii) short-term water deficit stress at 30% FC (ST 30% FC), and (iv) short-term water deficit stress at 30% FC followed by a recovery (ST 30% FC-Rec). Five individual replicates per genotype were randomly subjected to each treatment. Control plants were always maintained at 100% FC. For the other treatments, water irrigation was stopped until reaching 40% FC (ST 40% FC) or 30% FC (ST 30% FC and ST 30% FC-Rec). Once a specific FC was reached – after approximately 6 days for ST 40% FC and approximately 9 days for ST 30% and ST 30%-Rec – it was maintained. ST 30% FC-Rec was identical to ST 30% FC treatment, but a 2-day recovery until reaching 100% FC was applied. In all cases, the plants' water status was monitored every day, weighing the pots to maintain conditions at a specific FC by replacing evapo-transpired water. All measurements were performed in fully developed leaves of 40-day-old plants after their acclimation for 12 days to the specific conditions of each treatment.

Plants' water status

The Ψ_{pd} and Ψ_{md} values of each plant were determined in fully developed leaves using a pressure chamber (Model 600D; PMS Instrument Company, Albany, OR, USA). Additionally, those leaves used to determine Ψ_{md} were employed for the leaf *RWC* estimation. Thus, leaves were immediately weighed after measuring Ψ_{md}, obtaining the fresh weight (FW). Afterward, they were rehydrated overnight in distilled water under darkness at 4°C. The next morning, leaves were weighed to determine the turgid weight (TW). Finally, they were placed in an oven at 70°C for at least 72 h to obtain the dry weight (DW). From these measurements, *RWC* was calculated as follows:

$$RWC = \frac{FW - DW}{TW - DW} \times 100\%.$$

Foliar structure

The same leaves used to determine Ψ_{md} and *RWC* were also employed to estimate LMA and LD. Thus, when leaves were rehydrated, they were photographed to calculate the leaf area (LA) with ImageJ software (Wayne Rasband/NIH). Additionally, leaf thickness (LT) was estimated from five measurements per leaf avoiding main veins with a digital calliper. LMA was calculated using the following equation:

$$LMA = \frac{DW}{LA}.$$

Finally, LD was calculated as follows:

$$LD = \frac{LT}{LMA}.$$

Gas exchange and fluorescence measurements

A fully developed leaf per plant (the second or third leaf from the apex) acclimated to the water conditions imposed by a specific treatment was chosen to perform gas exchange and chlorophyll *a* fluorescence measurements using an infrared gas analyser coupled with a 2-cm^2 fluorometer chamber (Li-6400-40; Li-Cor Inc., Lincoln, NE, USA). The block temperature was kept at 25°C, the vapour pressure deficit (VPD) at around 1.5 kPa, the air flow rate at 300 μmol air min^{-1}, the light-saturating photosynthetically active radiation (PAR) at 1500 μmol m^{-2} sec^{-1} (90%/10% red/blue light) and the CO_2 ambient concentration (c_a) at 400 μmol CO_2 mol^{-1} air. When steady-state conditions were achieved (usually after 15–20 min), measurements of A_N, g_s, the CO_2 concentration at the substomatal cavity (c_i), and steady-state fluorescence (F_s) were conducted using a gas exchange system. Then, a saturating light flash was applied to obtain the maximum fluorescence (F_m'). From these values, the real quantum efficiency of photosystem II (Φ_{PSII}) was recorded. All previous measurements were made at 21% O_2. According to Valentini et al. (1995), light curves under non-

photorespiratory conditions (1% O_2) were drawn to calculate *ETR*. A seven-point curve was drawn by changing the light intensity in the cuvette from 1800 μmol m^{-2} sec^{-1} to 0 μmol m^{-2} sec^{-1}, being recorded after the stabilisation of the gas exchange system at each given light intensity (usually after 3 min). The remaining parameters (block temperature, VPD, flow rate, and c_a) were kept as described above. The R_{light} value was calculated at 21% O_2 as half the dark-adapted mitochondrial respiration after plants were exposed to darkness for 30 min (Niinemets et al., 2005). Based on these parameters, g_m was estimated by the variable *J* method (Harley et al., 1992) using the value for the CO_2 compensation point in the absence of respiration (Γ^*) reported for tomato by Hermida-Carrera et al. (2016). Given that cuticular properties can affect CO_2 diffusion (Boyer, 2015; Boyer et al., 1997; Flexas & Medrano, 2002), g_s and other parameters were calculated using leaf cuticular transpiration values reported in Galmés et al. (2011) (see Table S1).

Photosynthesis limitations analysis

Photosynthesis limitations were estimated following Grassi and Magnani (2005). *Absolute* stomatal (l_s), mesophyll (l_m) and biochemical (l_b) limitations were calculated per each genotype and treatment. Additionally, *relative* stomatal (*SL*), mesophyll (*ML*) and biochemical (*BL*) contributions to d*A*/*A* from a control to a water deficit stress state and during recovery were calculated assuming that the maximum A_N per genotype corresponded to that measured under control conditions.

Anatomical characterisation

At the end of gas exchange measurement, small portions of the leaves enclosed in the IRGA cuvette were cut, avoiding main veins. They were fixed under vacuum pressure with a 4% glutaraldehyde and 2% paraformaldehyde solution prepared in a 0.01 M phosphate buffer (pH 7.4). Then, samples were post-fixed for 2 h in 2% buffered osmium tetroxide and dehydrated by a graded ethanol series. Obtained pieces were embedded in LR resin (London Resin Company) and placed in an oven at 60°C for 48 h (Tomás et al., 2013; Tosens et al., 2012).

Semi-fine and ultra-fine cross-sections (0.8 μm and 90 nm, respectively) were cut with an ultramicrotome (Leica UC6, Vienna, Austria). Semi-fine cross-sections were dyed with 1% toluidine blue and photographed at 200× magnification with a digital camera (U-TVO.5XC; Olympus, Tokyo, Japan) coupled with an Olympus BX60 optic microscope. From these pictures, T_{leaf}, T_{mes}, and f_{ias} were calculated. Ultra-fine cross-sections were contrasted with uranyl acetate and lead citrate and photographed at 1500× and 30 000× magnifications with a transmission electron microscope (TEM H600; Hitachi, Tokyo, Japan). Pictures at 1500× magnifications were used to calculate T_{chl}, L_{chl}, S_m/S, S_c/S, and the S_c/S_m ratio. From pictures at 30 000× magnification, T_{cw} was calculated. Following Thain (1983), a cell curvature correction factor was determined performing an average length/width ratio of five cells per mesophyll type (palisade or spongy). Values for all parameters were averaged from 10 measurements performed in randomly selected cell structures using ImageJ. Finally, g_m was calculated based on anatomical particularities according to Tomás et al. (2013).

Pressure–volume curves

A fully developed leaf per plant adjacent to that employed for gas exchange measurements was chosen to draw pressure–volume (*P*–*V*) curves. Entire leaves (including the petiole) were cut to be rehydrated in distilled water under darkness overnight. The next morning, the leaf water potential was measured with a pressure chamber (Model 600D; PMS Instrument Company) and leaves were subsequently weighed. From *P*–*V* curves, the values of Ψ_{tlp}, RWC_{tlp}, π_o, ε, a_f, and C^*_{ft} were calculated (Sack et al., 2003; Sack & Pasquet-Kok, 2011).

Cell wall extraction and fractionation

The same leaves employed for gas exchange measurements were kept under darkness overnight to minimise starch accumulation. The following morning, around 700 mg of fresh foliar tissue per plant was cut in small portions to be boiled until bleaching in screwed-capped tubes filled with absolute ethanol. Then, they were cleaned twice with >95% acetone to obtain the AIR, an approximation of the total isolated cell wall material. AIRs were dried at room temperature and α-amylase digestion was performed to remove remaining starch. Then, three analytical replicates of each AIR weighing approximately 3 mg were hydrolysed with 2 M trifluoroacetic acid (TFA) at 121°C. After 1 h, samples were centrifuged, obtaining an aqueous supernatant and a pellet. While supernatants were directly employed for hemicelluloses and pectins quantifications, pellets were cleaned twice with distilled water and >95% acetone to eliminate TFA residues. The dry pellet (i.e., cellulose) was hydrolysed with 200 μl 72% sulphuric acid (w/v) for 1 h, diluted to 6 ml with distilled water, and heated at 121°C until degradation. Cellulose and hemicelluloses quantifications were performed by the phenol–sulphuric acid colorimetric procedure (Dubois et al., 1956). Absorbance was read at 490 nm and cellulose and hemicelluloses contents were calculated by interpolating values from a glucose calibration curve. Pectins quantification was performed by the colorimetric method of Blumenkrantz and Asboe-Hansen (1973) using 2-hydroxybiphenil as a reagent. Absorbance was read at 520 nm and the pectins content was estimated by interpolating values from a galacturonic acid calibration curve. A Multiskan Sky Microplate spectrophotometer (ThermoFisher Scientific Inc.) was used in all cases.

Statistical analysis

Prior to performing statistical analysis, the Thompson test was used to detect and eliminate outliers in the database. Then, two-way analysis of variance (ANOVA) followed by a least significant difference (LSD) test was performed to identify statistically significant (***$P < 0.001$; **$P < 0.01$; *$P < 0.05$) 'genotype', 'treatments', and 'genotypes × treatment' effects. A PCA was made considering mean values per parameter and treatment for each treatment to analyse the effects of distinct treatments and the interactions between distinct parameters. Also, Pearson correlation matrices were constructed for each genotype to find correlations between all tested parameters, being significant and highly significant when $P < 0.05$ and $P < 0.01$, respectively. Finally, linear regression analysis was addressed to analyse correlations between photosynthetic, leaf water relations, anatomical, and cell wall composition parameters using mean values per genotype and treatment. All these analyses were performed with R software (ver. 3.2.2; R Core Team, Vienna, Austria).

AUTHOR CONTRIBUTIONS

MR-O, JB, and JF conceived and designed the study; MR-O and MF-P conducted the experiments; MR-O and JF performed the data analysis; and MR-O wrote the first version of the manuscript with input from all co-authors.

ACKNOWLEDGEMENTS

We thank Dr Miquel À. Conesa for his help with genotype selection. This work was supported by the project PGC2018-093824-B-

C41 from the Ministerio de Economía y Competitividad (MINECO, Spain) and the ERDF (FEDER). MR-O was supported by a pre-doctoral fellowship (FPU16/01544) from MINECO.

CONFLICTS OF INTEREST

The authors declare no conflicts of interest.

DATA AVAILABILITY STATEMENT

The data supporting the findings of this study are available from the corresponding author upon request.

SUPPORTING INFORMATION

Additional Supporting Information may be found in the online version of this article.

Figure S1. Anatomical characteristics of the studied genotypes from semi-fine (left) and ultra-fine (right) cross-sections taken at 200× and at 30 000× magnifications, respectively. From top to bottom, all pictures included in the four first lines represent non-long shelf-life (nLSL) genotype particularities, whereas the last four lines show LSL genotype traits. CL conditions correspond to A, I and E, M; ST 40% FC to B, J and F, N; ST 30% FC to C, K and G, O; and ST 30% FC-Rec to D, L and H, P. Black scale bars in semi-fine cross-sections = 200 μm. The detailed quantitative analyses of all studied anatomical parameters are shown in Tables 4 and 5.

Table S1. Summary of the cuticular conductance (g_{cut}) values that were used to recalculate g_s and, consequently, c_i, g_m, and WUE_i in the tested genotypes. These g_{cut} values were obtained after the conversion of leaf cuticular transpiration (t_{cut}) values reported in Galmés et al. (2011). The same t_{cut} and, consequently, g_{cut} values were used for both genotypes since they presented tomato leaf morphology. However, different values were employed according to well-watering or water deficit stress treatments.

Table S2. Mesophyll conductance (g_m) calculated from fluorescence and anatomical measurements performed in tomato non-long shelf-life (nLSL) and long shelf-life (LSL) genotypes subjected to different conditions (control [CL], short-term water deficit stress at 40% FC [ST 40% FC], short-term water deficit stress at 30% FC [ST 30% FC], and short-term water deficit stress at 30% FC followed by recovery [ST 30% FC-Rec]). While g_m_fluorescence was calculated according to Harley et al. (1992), g_m_anatomy was estimated following Tomás et al. (2013). Mean values ± SE values are shown. Genotype (G) and treatment (T) effects were quantified by two-way ANOVA and differences between groups were analysed by LSD test. $n = 5$ in all cases.

Table S3. Pearson correlation matrix of physiological, leaf water relation, cell wall, and anatomical parameters measured in the *S. lycopersicum* nLSL genotype across all experimental conditions. Values in italics and bold indicate significant ($P < 0.05$) and highly significant ($P < 0.01$) correlation coefficients, respectively.

Table S4. Pearson correlation matrix of physiological, leaf water relation, cell wall, and anatomical parameters measured in the *S. lycopersicum* LSL genotype across all experimental conditions. Values in italics and bold indicate significant ($P < 0.05$) and highly significant ($P < 0.01$) correlation coefficients, respectively.

REFERENCES

Abrams, M.D. (1990) Adaptations and responses to drought in *Quercus* species of North America. *Tree Physiology*, **7**, 227–238. Available from: https://doi.org/10.1093/treephys/7.1-2-3-4.227

Anderson, C.T. & Kieber, J.J. (2020) Dynamic construction, perception, and remodelling of plant cell walls. *Annual Review of Plant Biology*, **71**, 39–69. Available from: https://doi.org/10.1146/annurev-arplant-081519-035846

Blumenkrantz, N. & Asboe-Hansen, G. (1973) New method for quantitative determination of uronic acids. *Analytical Biochemistry*, **54**, 484–489. Available from: https://doi.org/10.1016/0003-2697(73)90377-1

Bota, J., Conesa, M.À., Ochogavía, J.M., Medrano, H., Francis, D.M. & Cifre, J. (2014) Characterization of a landrace collection for Tomàtiga de Ramellet (*Solanum lycopersicum* L.) from the Balearic Islands. *Genetic Resources and Crop Evolution*, **61**, 1131–1146. Available from: https://doi.org/10.1007/s10722-014-0096-3

Boyer, J.S. (2015) Impact of cuticle on calculations of the CO_2 concentration inside leaves. *Planta*, **242**, 1405–1412. Available from: https://doi.org/10.1007/s00425-015-2378-1

Boyer, J.S., Wong, S.C. & Farquhar, G.D. (1997) CO_2 and water vapour exchange across leaf cuticle (epidermis) at various water potentials. *Plant Physiology*, **114**, 185–191. Available from: https://doi.org/10.1104/pp.114.1.185

Carpita, N.C. (1996) Structure and biogenesis of the cell walls of grasses. *Annual Review of Plant Physiology and Plant Molecular Biology*, **47**, 445–476. Available from: https://doi.org/10.1146/annurev.arplant.47.1.445

Carpita, N.C. & McCann, M.C. (2002) The functions of cell wall polysaccharides in composition and architecture revealed through mutations. *Plant and Soil*, **247**, 71–80. Available from: https://doi.org/10.1023/A:1021115300942

Cebolla-Cornejo, J., Rosselló, S. & Nuez, F. (2013) Phenotypic and genetic diversity of Spanish tomato landraces. *Scientia Horticulturae*, **162**, 150–164. Available from: https://doi.org/10.1016/j.scienta.2013.07.044

Chaves, M.M., Flexas, J. & Pinheiro, C. (2009) Photosynthesis under drought and salt stress: regulation mechanisms from whole plant to cell. *Annals of Botany*, **103**, 551–560. Available from: https://doi.org/10.1093/aob/mcn125

Clemente-Moreno, M.J., Gago, J., Díaz-Vivancos, P., Bernal, A., Miedes, E., Bresta, P. *et al.* (2019) The apoplastic antioxidant system and altered cell wall dynamics influence mesophyll conductance and the rate of photosynthesis. *The Plant Journal*, **99**, 1031–1046. Available from: https://doi.org/10.1111/tpj.14437

Conesa, M.À., Fullana-Pericàs, M., Granell, A. & Galmés, J. (2020) Mediterranean long shelf-life landraces: an untapped genetic resource for tomato improvement. *Frontiers in Plant Science*, **10**, 1651. Available from: https://doi.org/10.3389/fpls.2019.01651

Conesa, M.À., Galmés, J., Ochogavía, J.M., March, J., Jaume, J., Martorell, A. *et al.* (2014) The postharvest tomato fruit quality of long shelf-life Mediterranean landraces is substantially influenced by irrigation regimes. *Postharvest Biology and Technology*, **93**, 114–121. Available from: https://doi.org/10.1016/j.postharvbio.2014.02.014

Cortés-Olmos, C., Valcárcel, J.V., Rosselló, J., Díez, M.J. & Cebolla-Cornejo, J. (2015) Traditional eastern Spanish varieties of tomato. *Science in Agriculture*, **5**, 420–431. Available from: https://doi.org/10.1590/0103-9016-2014-0322

Cosgrove, D.J. (2005) Growth of the plant cell wall. *Nature Reviews. Molecular Cell Biology*, **6**, 850–861. Available from: https://doi.org/10.1038/nrm1746

Cosgrove, D.J. (2018) Diffusive growth of plant cell walls. *Plant Physiology*, **176**, 16–27. Available from: https://doi.org/10.1104/pp.17.01541

Dodd, I.C. (2007) Soil moisture heterogeneity during deficit irrigation alters root-to-shoot signalling of abscisic acid. *Functional Plant Biology*, **34**, 439–448. Available from: https://doi.org/10.1071/FP07009

Dubois, M., Gilles, K.A., Hamilton, J.K., Rebers, P.A. & Smith, F. (1956) Colorimetric method for determination of sugars and related substances. *Analytical Chemistry*, **28**, 350–356. Available from: https://doi.org/10.1021/ac60111a017

Evans, L.T. (1997) Adapting and improving crops: the endless task. *Philosophical Transactions of the Royal Society B: Biological Sciences*, **352**, 901–906. Available from: https://doi.org/10.1098/rstb.1997.0069

FAO. (2021) htttp://fao.org/faostat (Accessed 8th May 2021).

Flexas, J., Bota, J., Loreto, F., Cornic, G. & Sharkey, T.D. (2004) Diffusive and metabolic limitations to photosynthesis under drought and salinity in C_3 plants. *Plant Biology*, **6**, 269–279. Available from: https://doi.org/10.1055/s-2004-820867

Flexas, J. & Carriquí, M. (2020) Photosynthesis and photosynthetic efficiencies along the terrestrial plant's phylogeny: lessons for improving crop

photosynthesis. *The Plant Journal*, **101**, 964–978. Available from: https://doi.org/10.1111/tpj.14651

Flexas, J., Clemente-Moreno, M.J., Bota, J., Brodribb, T.J., Gago, J., Mizokami, Y. *et al.* (2021) Cell wall thickness and composition are involved in photosynthetic limitation. *Journal of Experimental Botany*, **72**, 3971–3986. Available from: https://doi.org/10.1093/jxb/erab144

Flexas, J. & Medrano, H. (2002) Energy dissipation in C_3 plants under drought. *Functional Plant Biology*, **29**, 1209–1215. Available from: https://doi.org/10.1071/FP02015

Flexas, J., Niinemets, Ü., Gallé, A., Barbour, M.M., Centritto, M., Díaz-Espejo, A. *et al.* (2013) Diffusional conductances to CO_2 as a target for increasing photosynthesis and photosynthetic water-use efficiency. *Photosynthesis Research*, **117**, 45–59. Available from: https://doi.org/10.1007/s11120-013-9844-z

Flores, P., Sánchez, E., Fenoll, J. & Hellin, P. (2017) Genotypic variability of carotenoids in traditional tomato cultivars. *Food Research International*, **100**, 510–516. Available from: https://doi.org/10.1016/j.foodres.2016.07.014

Fullana-Pericàs, M., Conesa, M.À., Douthe, C., El Aou-ouad, H., Ribas-Carbó, M. & Galmés, J. (2019) Tomato landraces as a source to minimize yield losses and improve fruit quality under water deficit conditions. *Agricultural Water Management*, **223**, 105722. Available from: https://doi.org/10.1016/j.agwat.2019.105722

Fullana-Pericàs, M., Conesa, M.À., Soler, S., Ribas-Carbó, M., Granell, A. & Galmés, J. (2017) Variations of leaf morphology, photosynthetic traits and water-use efficiency in Western-Mediterranean tomato landraces. *Photosynthetica*, **55**, 121–133. Available from: https://doi.org/10.1007/s11099-016-0653-4

Gago, J., Carriquí, M., Nadal, M., Clemente-Moreno, M.J., Coopman, R.E., Fernie, A.R. *et al.* (2019) Photosynthesis optimized across land plant phylogeny. *Trends in Plant Science*, **24**, 947–958. Available from: https://doi.org/10.1016/j.tplants.2019.07.002

Galmés, J., Conesa, M.À., Ochogavía, J.M., Perdomo, J.A., Francis, D.M., Ribas-Carbó, M. *et al.* (2011) Physiological and morphological adaptations in relation to water use efficiency in Mediterranean accessions of *Solanum lycopersicum*. *Plant, Cell & Environment*, **34**, 245–260. Available from: https://doi.org/10.1111/j.1365-3040.2010.02239.x

Galmés, J., Ochogavía, J.M., Gago, J., Roldán, E.J., Cifre, J. & Conesa, M.À. (2013) Leaf responses to drought stress in Mediterranean accessions of *Solanum lycopersicum*: anatomical adaptations in relation to gas exchange parameters. *Plant, Cell & Environment*, **36**, 920–935. Available from: https://doi.org/10.1111/pce.12022

Grassi, G. & Magnani, F. (2005) Stomatal, mesophyll conductance and biochemical limitations to photosynthesis as affected by drought and leaf ontogeny in ash and oak trees. *Plant, Cell & Environment*, **28**, 834–849. Available from: https://doi.org/10.1111/j.1365-3040.2005.01333.x

Hanba, Y., Kogami, H. & Terashima, I. (2002) The effect of growth irradiance on leaf anatomy and photosynthesis in *acer* species differing in light demand. *Plant, Cell & Environment*, **25**, 1021–1030. Available from: https://doi.org/10.1046/j.1365-3040.2002.00881.x

Harley, P.C., Loreto, F., Di Marco, G. & Sharkey, T.D. (1992) Theoretical considerations when estimating the mesophyll conductance to CO_2 flux by the analysis of the response of photosynthesis to CO_2. *Plant Physiology*, **98**, 1429–1436. Available from: https://doi.org/10.1104/pp.98.4.1429

Hermida-Carrera, C., Kapralov, M.V. & Galmés, J. (2016) Rubisco catalytic properties and temperature response in crops. *Plant Physiology*, **171**, 2549–2561. Available from: https://doi.org/10.1104/pp.16.01846

Houston, K., Tucker, M.R., Chowdhury, J., Shirley, N. & Little, A. (2016) The plant cell wall: a complex and dynamic structure as revealed by the responses of genes under stress conditions. *Frontiers in Plant Science*, **7**, 984. Available from: https://doi.org/10.3389/fpls.2016.00984

Kubiske, M.E. & Abrams, M.D. (1991) Rehydration effects on pressure–volume relationships in four temperate woody species: variability with site, time of season and drought conditions. *Oecologia*, **85**, 537–542. Available from: https://doi.org/10.1007/BF00323766

Lo Gullo, M.A. & Salleo, S. (1988) Different strategies of drought resistance in three Mediterranean sclerophyllous trees growing in the same environmental conditions. *The New Phytologist*, **108**, 267–276. Available from: https://doi.org/10.1111/j.1469-8137.1988.tb04162.x

Long, S.P., Zhu, X.G., Naidu, S.L. & Ort, D.R. (2006) Can improvement in photosynthesis increase crop yields? *Plant, Cell & Environment*, **29**, 315–330. Available from: https://doi.org/10.1111/j.1365-3040.2005.01493.x

Manzo, N., Pizzolongo, F., Meca, G., Aiello, A., Marchetti, N. & Romano, R. (2018) Comparative chemical compositions of fresh and stored vesuvian PDO "Pomodorino Del Piennolo" tomato and the ciliegino variety. *Molecules*, **23**, 2871. Available from: https://doi.org/10.3390/molecules23112871

Mickelbart, M.V., Hasegawa, P.M. & Bailey-Serres, J. (2015) Genetic mechanisms of abiotic stress tolerance that translate to crop yield stability. *Nature Reviews. Genetics*, **16**, 237–251. Available from: https://doi.org/10.1038/nrg3901

Morison, J.I.L., Baker, N.R., Mullineaux, P.M. & Davies, W.J. (2008) Improving water use in crop production. *Philosophical Transactions of the Royal Society B: Biological Sciences*, **363**, 639–658. Available from: https://doi.org/10.1098/rstb.2007.2175

Nadal, M. & Flexas, J. (2019) Variation in photosynthetic characteristics with growth form in a water-limited scenario: implications for assimilation rated and water use efficiency in crops. *Agricultural Water Management*, **216**, 457–472. Available from: https://doi.org/10.1016/j.agwat.2018.09.024

Nadal, M., Flexas, J. & Gulías, J. (2018) Possible link between photosynthesis and leaf modulus of elasticity among vascular plants: a new player in leaf traits relationships? *Ecology Letters*, **21**, 1372–1379. Available from: https://doi.org/10.1111/ele.13103

Nadal, M., Roig-Oliver, M., Bota, J. & Flexas, J. (2020) Leaf age-dependent elastic adjustment and photosynthetic performance under drought stress in *Arbutus unedo* seedlings. *Flora*, **271**, 151662. Available from: https://doi.org/10.1016/j.flora.2020.151662

Niinemets, Ü., Cescatti, A., Rodeghiero, M. & Tosens, T. (2005) Leaf internal diffusion conductance limits photosynthesis more strongly in older leaves of Mediterranean evergreen broadleaved species. *Plant, Cell & Environment*, **28**, 1552–1566. Available from: https://doi.org/10.1111/j.1365-3040.2005.01392.x

Park, Y.B. & Cosgrove, D.J. (2012) Changes in cell wall biomechanical properties in the xyloglucan-deficient *xxt1*/*xxt2* mutant of *Arabidopsis*. *Plant Physiology*, **158**, 465–475. Available from: https://doi.org/10.1104/pp.111.189779

Peguero-Pina, J.J., Sancho-Knapik, D. & Gil-Pelegrín, E. (2017) Ancient cell structural traits and photosynthesis in today's environment. *Journal of Experimental Botany*, **68**, 1389–1392. Available from: https://doi.org/10.1093/jxb/erx081

Pérez-Martín, A., Michelazzo, C., Torres-Ruiz, J.M., Flexas, J., Fernández, J.E., Sebastiani, L. *et al.* (2014) Regulation of photosynthesis and stomatal and mesophyll conductance under water stress and recovery in olive trees: correlation with gene expression of carbonic anhydrase and aquaporins. *Journal of Experimental Botany*, **65**, 3143–3156. Available from: https://doi.org/10.1093/jxb/eru160

Roig-Oliver, M., Bresta, P., Nadal, M., Liakopoulos, G., Nikolopoulos, D., Karabourniotis, G. *et al.* (2020) Cell wall composition and thickness affect mesophyll conductance to CO_2 diffusion in *Helianthus annuus* under water deprivation. *Journal of Experimental Botany*, **71**, 7198–7209. Available from: https://doi.org/10.1093/jxb/eraa413

Roig-Oliver, M., Bresta, P., Nikolopoulos, D., Bota, J. & Flexas, J. (2021) Dynamic changes in cell wall composition of mature sunflower leaves under distinct water regimes affect photosynthesis. *Journal of Experimental Botany*, **72**, 7863–7875. Available from: https://doi.org/10.1093/jxb/erab372

Roig-Oliver, M., Fullana-Pericàs, M., Bota, J. & Flexas, J. (2021) Adjustments in photosynthesis and leaf water relations are related to changes in cell wall composition in *Hordeum vulgare* and *Triticum aestivum* subjected to water deficit stress. *Plant Science*, **311**, 111015. Available from: https://doi.org/10.1016/j.plantsci.2021.111015

Roig-Oliver, M., Nadal, M., Bota, J. & Flexas, J. (2020) *Ginkgo biloba* and *Helianthus annuus* show different strategies to adjust photosynthesis, leaf water relations, and cell wall composition under water deficit stress. *Photosynthetica*, **58**, 1098–1106. Available from: https://doi.org/10.32615/ps.2020.063

Roig-Oliver, M., Nadal, M., Clemente-Moreno, M.J., Bota, J. & Flexas, J. (2020) Cell wall components regulate photosynthesis and leaf water relations of *Vitis vinifera* cv. Grenache acclimated to contrasting environmental conditions. *Journal of Plant Physiology*, **244**, 153084. Available from: https://doi.org/10.1016/j.jplph.2019.153084

Rui, Y. & Dinneny, J.R. (2019) A wall with integrity: surveillance and maintenance of the plant cell wall under stress. *The New Phytologist*, **225**, 1428–1439. Available from: https://doi.org/10.1111/nph.16166

Sack, L., Cowan, P.D., Jaikumar, N. & Holbrook, N.M. (2003) The 'hydrology' of leaves: coordination of structure and function intemperate woody

species. *Plant, Cell & Environment*, **26**, 1343–1356. Available from: https://doi.org/10.1046/j.0016-8025.2003.01058.x

Sack, L. & Pasquet-Kok, J. (2011) Leaf pressure-volume curve parameters. Prometheus Wiki. http://prometheuswiki.org/tiki-pagehistory.php?page=Leaf%20pressure-volume%20curve%20parameters&preview=16 (Accessed 28th March 2021)

Saladié, M., Matas, A.J., Isaacson, T., Jenks, M.A., Goodwin, S.M., Niklas, K.J. *et al.* (2007) A reevaluation of the key factors that influence tomato fruit softening and integrity. *Plant Physiology*, **144**, 1012–1028. Available from: https://doi.org/10.1104/pp.107.097477

Saradadevi, R., Bramley, H., Palta, J.A., Edwards, E. & Siddique, K.H.M. (2015) Root biomass in the upper layer of the soil profile is related to the stomatal response of wheat as the soil dries. *Functional Plant Biology*, **43**, 62–74. Available from: https://doi.org/10.1071/FP15216

Schultz, H.R. (2016) Global climate change, sustainability, and some challenges for grape and wine production. *Journal of Wine Economics*, **11**, 181–200. Available from: https://doi.org/10.1017/jwe.2015.31

Sobrado, M.A. & Turner, N.C. (1983) A comparison of the water relations characteristics of *Helianthus annuus* and *Helianthus petiolaris* when subjected to water deficits. *Oecologia*, **58**, 309–313. Available from: https://doi.org/10.1007/BF00385228

Sweet, W.J., Morrison, J.C., Labavitch, J. & Matthews, M.A. (1999) Altered synthesis and composition of cell wall of grape (*Vitis vinifera* L.) leaves during expansion and growth-inhibiting water deficits. *Plant & Cell Physiology*, **31**, 407–414. Available from: https://doi.org/10.1093/oxfordjournals.pcp.a077924

Tenhaken, R. (2015) Cell wall remodeling under abiotic stress. *Frontiers in Plant Science*, **5**, 771. Available from: https://doi.org/10.3389/fpls.2014.00771

Thain, J.F. (1983) Curvature correlation factors in the measurements of cell surface areas in plant tissues. *Journal of Experimental Botany*, **34**, 87–94. Available from: https://doi.org/10.1093/jxb/34.1.87

Tholen, D., Boom, C., Noguchi, K., Ueda, S., Katase, T. & Terashima, I. (2008) The chloroplast avoidance response decreases internal conductance to CO_2 diffusion in *Arabidopsis thaliana* leaves. *Plant, Cell & Environment*, **11**, 1688–1700. Available from: https://doi.org/10.1111/j.13653040.2008.01875.x

Tilman, D., Cassman, K.G., Matson, P.A., Naylor, R. & Polasky, S. (2002) Agricultural sustainability and intensive production practices. *Nature*, **418**, 671–677. Available from: https://doi.org/10.1038/nature01014

Tomás, M., Flexas, J., Copolovici, L., Galmés, J., Hallik, L., Medrano, H. *et al.* (2013) Importance of leaf anatomy in determining mesophyll diffusion conductance to CO_2 across species: quantitative limitations and scaling up by models. *Journal of Experimental Botany*, **64**, 2269–2281. Available from: https://doi.org/10.1093/jxb/ert086

Tosens, T., Niinemets, Ü., Vislap, V., Eichelmann, H. & Castro-Díez, P. (2012) Developmental changes in mesophyll diffusion conductance and photosynthetic capacity under different light and water availabilities in *Populus tremula*: how structure constrains function. *Plant, Cell & Environment*, **35**, 839–856. Available from: https://doi.org/10.1111/j.1365–3040.2011.02457.x

Tranchida-Lombardo, V., Aiese Cigliano, R., Anzar, I., Landi, S., Palombieri, S., Colantuono, C. *et al.* (2018) Whole-genome re-sequencing of two Italian tomato landraces reveals sequence variations in genes associated with stress tolerance, fruit quality and long shelf-life traits. *DNA Research*, **25**, 149–160. Available from: https://doi.org/10.1093/dnares/dsx045

Tucker, M.R., Lou, H., Aubert, M.K., Wilkinson, L.G., Little, A., Houston, K. *et al.* (2018) Exploring the role of cell wall-related genes and polysaccharides during plant development. *Plants*, **7**, 42. Available from: https://doi.org/10.3390/plants7020042

Turner, N.C. (2018) Turgor maintenance by osmotic adjustment: 40 years of progress. *Journal of Experimental Botany*, **69**, 3223–3233. Available from: https://doi.org/10.1093/jxb/ery181

Valentini, R., Epron, D., Angelis, P.D., Matteucci, G. & Dreyer, E. (1995) In situ estimation of net CO_2 assimilation, photosynthetic electron flow and photorespiration of Turkey oak (*Q. cerris* L.) leaves: diurnal cycles under different water supply. *Plant, Cell & Environment*, **18**, 631–664. Available from: https://doi.org/10.1111/j.1365-3040.1995.tb00564.x

Wu, A., Hammer, G.L., Doherty, A., von Caemmerer, S. & Farquhar, G.D. (2019) Quantifying impacts of enhancing photosynthesis on crop yield. *Nature Plants*, **5**, 380–388. Available from: https://doi.org/10.1038/s41477-019-0398-8

Xiong, D. & Nadal, M. (2020) Linking water relations and hydraulics with photosynthesis. *The Plant Journal*, **101**, 800–815. Available from: https://doi.org/10.1111/tpj.14595

Ye, M., Zhang, Z., Huang, G., Xiong, Z., Peng, S. & Li, Y. (2020) High leaf mass per area *Oryza* genotypes invest more leaf mass to cell wall and show a low mesophyll conductance. *AoB Plants*, **12**, plaa028. Available from: https://doi.org/10.1093/aobpla/plaa028